VIP Bioorganometallic Chemistry

DOI: 10.1002/anie.201000682

Iridium Complex with Antiangiogenic Properties**

*Alexander Wilbuer, Danielle H. Vlecken, Daan J. Schmitz, Katja Kräling, Klaus Harms, Christoph P. Bagowski, and Eric Meggers**

Substitutionally inert metal complexes are promising emerging scaffolds for targeting enzyme active sites.[1] Over the last several years, our research group has demonstrated that inert ruthenium(II) complexes can serve as highly selective nanomolar and even picomolar inhibitors of protein kinases.[2] Octahedral metal coordination geometries in particular offer new gateways to design rigid, globular molecules with defined shapes that can fill protein pockets such as enzyme active sites in a unique fashion (Figure 1).[3] However, the large number of possible stereoisomers does not only provide new structural opportunities (e.g. the complex illustrated in Figure 1 can form up to 24 stereoisomers if the ligands A–D differ), but also poses a formidable challenge because of the limited ability to control the stereochemistry in the course of ligand exchange reactions.[4] A continued progress in this area of inorganic medicinal chemistry therefore requires the development of strategies for the stereocontrolled synthesis of octahedrally coordinated metal complexes.

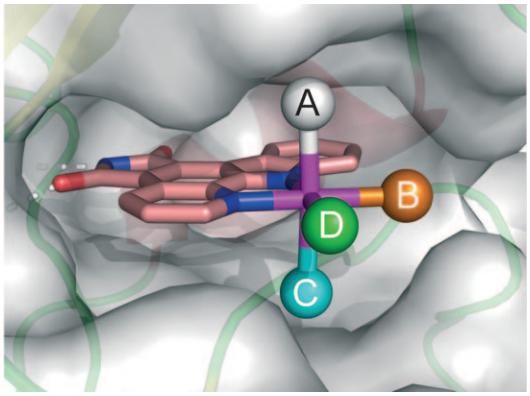

Figure 1. Illustration of an octahedral pyridocarbazole metal complex bound to the active site of a protein kinase. The coordinating ligands A–D are capable of controlling kinase affinities and selectivities, if arranged properly.

[*] A. Wilbuer, K. Kräling, Dr. K. Harms, Prof. Dr. E. Meggers
Fachbereich Chemie, Philipps-Universität Marburg
Hans-Meerwein-Strasse, 35032 Marburg (Germany)
Fax: (+49) 6421-282-2189
E-mail: meggers@chemie.uni-marburg.de
D. H. Vlecken, D. J. Schmitz, Prof. Dr. C. P. Bagowski
Institute of Biology, Leiden University
Wassenaarseweg 64, 2333 AL Leiden (The Netherlands)

[**] Financial support was provided by the DFG (FOR630).

Supporting information for this article is available on the WWW under http://dx.doi.org/10.1002/anie.201000682.

Although most of our previous efforts were focused on ruthenium(II) complexes, we envisioned that octahedral iridium(III) complexes might be attractive scaffolds for two reasons: First, coordinative bonds with Ir^{III} tend to be very inert[5] and therefore Ir^{III} complexes should be able to serve as stable scaffolds for the design of enzyme inhibitors.[6,7] Second, octahedral Ir^{III} complexes can be accessed from square-planar Ir^{I} complexes by stereoselective oxidative addition reactions.[8] This factor provides a powerful tool to control the stereochemistry of octahedral Ir^{III} complexes.

Herein, we present the discovery of a bioactive octahedral iridium(III) complex, synthesized through oxidative addition as the key synthetic step. The organometallic compound functions as a nanomolar and selective inhibitor of the protein kinase Flt4 (Fms-related tyrosine kinase 4), also known as VEGFR3 (vascular endothelial growth factor receptor 3).[9] Flt4 is involved in angiogenesis and lymphangiogenesis[9] and we demonstrate that this nontoxic organoiridium compound can indeed interfere with the development of blood vessels in vivo in two different zebrafish angiogenesis models.

We started with investigating the synthesis of iridium complexes containing our recently developed pyridocarbazole pharmacophore bidentate ligand that targets the complexes to the ATP-binding site of protein kinases (Figure 1). For initial studies we used pyridocarbazoles **1a–c** bearing different substituents R at the maleimide nitrogen atom (**a**: Bn, **b**: TBS, **c**: CH_3). Accordingly, heterocycles **1a–c** were treated with [{IrCl(cod)}$_2$] in MeCN/MeOH (2:1) in the presence of K_2CO_3 to afford the iridium(I) complexes **2a–c** in high yields (90–95%, Scheme 1). These slightly air-sensitive square-planar complexes efficiently undergo oxidative addition. For example, the reaction of **2a**,**b** with freshly distilled CH_3I in the dark provided the stable octahedral complexes **3a**,**b** stereoselectively as the *trans* oxidative addition products (89% and 92%, respectively).[10] Similarly, the treatment of **2a–c** with I_2 afforded the octahedral complexes **4a–c** (73–92%), whereas the reaction of **2b** with first (trifluoromethyl)dibenzothiophenium tetrafluoroborate[11] followed by TBAC, afforded the complex **5** (29%) containing a stable Ir–CF_3 bond. A crystal structure of complex **4a** is shown in Figure 2 and reveals the *trans* coordination of iodine. Importantly, the iodide ligands in **4a** can further be subjected to substitution chemistry, as exemplified by the conversion into the dichloride complex **6** upon treatment with TBAC (88%). Encouraged by these results, we synthesized in an analogous fashion a small library of iridium complexes **7–11** bearing unprotected maleimide moieties. The free maleimide nitrogen atoms are essential for being capable of forming two canonical hydrogen bonds with the hinge region of the ATP-binding site of protein kinases (Scheme 1).

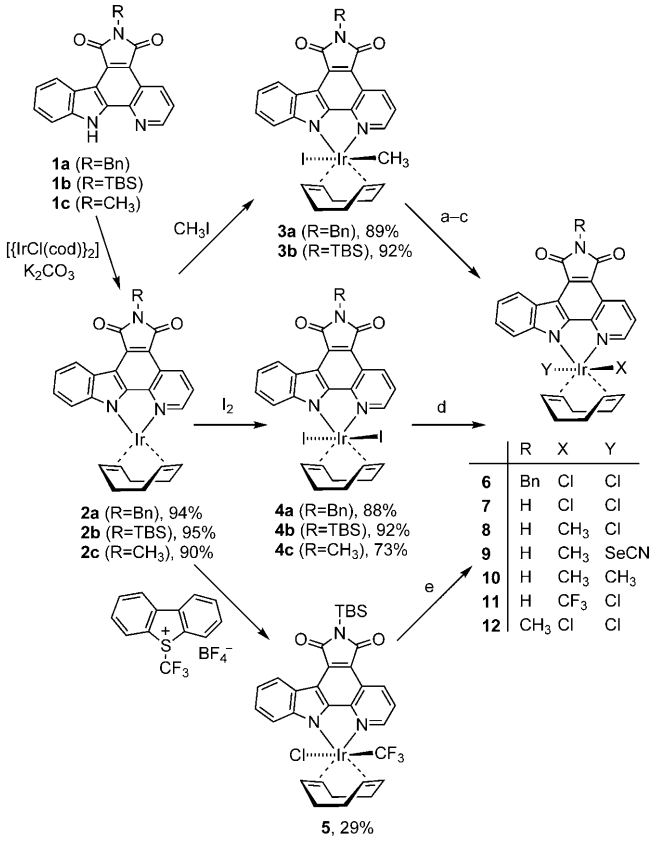

Scheme 1. Synthesis of octahedral iridium complexes used in this study through oxidative addition as the key step. Reagents and conditions: a) TBAC, THF, 79% of **8**; b) KSeCN, DMF, 83% of **9**; c) MeMgBr, CuI, THF, 63%; then TBAF, CH_2Cl_2, 73% of **10**; d) TBAC, THF, 88% of **6**, 59% of **7**, and 71% of **12**; e) TBAC, THF, microwave (70 °C, 17 min, 20 watts), 50% of **11**. Bn = benzyl, cod = cycloocta-1,5-diene, DMF = *N*,*N*-dimethylformamide, TBAC = tetrabutyl ammonium chloride, TBS = *tert*-butyldimethylsilyl, THF = tetrahydrofuran.

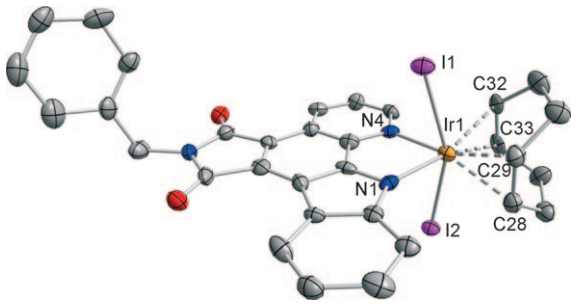

Figure 2. ORTEP representation (50% thermal ellipsoids) of the crystal structure of complex **4a**. Selected bond lengths [Å]: N1–Ir1 2.070(6), N4–Ir1 2.122(6), C28–Ir1 2.240(8), C29–Ir1 2.251(7), C32–Ir1 2.222(7), C33–Ir1 2.252(7), I1–Ir1 2.733(6), I2–Ir1 2.714(6). Selected bond angles [°]: N1-Ir1-I2 82.29(16), N4-Ir1-I2 81.44(16), N1-Ir1-I1 80.42(16), N4-Ir1-I1 81.15(16), I2-Ir1-I1 157.12(2).

To quickly evaluate the kinase inhibition properties of this class of iridium complexes, we selected compound **8** as a representative member and screened it against a panel of protein kinases. As a result, at a concentration of 1 μM of **8** and 10 μM of ATP only 12 out of 263 kinases showed activities below 25% (see the Supporting Information). Intriguingly, the receptor tyrosine kinase Flt4, which was not selectively inhibited by any of the previously reported ruthenium scaffolds,[1,2] displayed under these conditions only an activity of 2%. We therefore chose Flt4 for further studies and tested the small library of iridium compounds **7**–**11** against this kinase by determining the concentrations of **7**–**11** at which Flt4 kinase activity was lowered to 50% (the IC_{50} value) at an ATP concentration of 100 μM. As expected, ligands X and Y of compounds **7**–**11** (Scheme 1) turned out to have a profound effect on the inhibition properties. Whereas compound **8** displayed an IC_{50} value of (211 ± 23) nM, the more hydrophobic dimethyl derivative **10** had a significantly lower potency ($IC_{50} = 1007 \pm 129$ nM). Replacing the CH_3 group in **8** by a CF_3 group also lowered affinity with an IC_{50} value of (369 ± 68) nM for **11**. Furthermore, as seen for compound **9**, substituting the chloride group for a selenocyanate group decreased the inhibition potency slightly compared to complex **8** ($IC_{50} = (326 \pm 52)$ nM for complex **9**). However, complex **7** with X = Y = Cl showed a significantly improved activity with an IC_{50} value of (123 ± 14) nM, thus being almost an order of magnitude more potent against Flt4 than the related dimethyl derivative **10**. From these data it becomes apparent that the ligands X and Y have a profound effect on the kinase inhibition properties with the small library of organoiridium complexes **7**–**11** already spanning across an activity range of almost one order of magnitude. This observation is consistent with previous studies of organometallic protein kinase inhibitors which revealed the importance of the ligand pointing towards the glycine-rich loop for kinase inhibition (ligand A in Figure 1).[12] Our results thus demonstrate that oxidative addition provides a convenient synthetic tool to quickly scan ligands in the positions perpendicular to the pyridocarbazole moiety (ligands A and D in Figure 1), which to our opinion is a unique feature of this iridium scaffold.

For the purpose of designing molecular probes for chemical biology, the selectivity of a compound is one of its most important single features. This is especially a challenge for members of large enzyme families such as protein kinases with more than 500 putative protein kinase genes encoded in the human genome. Nevertheless, iridium complex **7** displays a remarkable degree of selectivity for Flt4 over other protein kinases. Figure 3 shows the results of a screening of complex **7** against a panel of 229 human wild-type protein kinases at a concentration of 100 nM (10 μM ATP). Out of the 229 protein kinases, 224 kinases remained an activity of more than 50%, including other members of the VEGFR family such as VEGFR1 (also known as Flt1, 62% activity at 100 nM **7**, 10 μM ATP) and VEGFR2 (also known as KDR, 95% activity at 100 nM **7**, 10 μM ATP). On the other hand, only 5 kinases, including Flt4, were inhibited by more than 50% under these conditions. The IC_{50} measurements with some of these kinases at the biologically more relevant concentration of 250 μM ATP confirmed the exquisite selectivity of **7** for Flt4: Pim1 ($IC_{50} = 560 \pm 8$ nM) and GSK3 (measured for the more potent α-isoform: $IC_{50} = 338 \pm 42$ nM) are inhibited with potencies which are lower compared to the inhibition of Flt4 by **7**

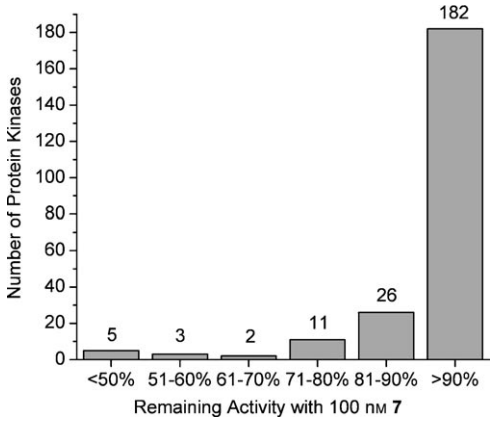

Figure 3. Selectivity profile of iridium compound **7** in a panel of 229 human wild-type protein kinases. Determined by Millipore (KinaseProfiler) at a concentration of 10 μM ATP. Remaining activities are mean values from duplicate measurements. Selectivity comparison within the VEGFR family (remaining activities at 100 nM **7**): Flt1 (VEGFR1) 62%, KDR (VEGFR2) 95%, Flt4 (VEGFR3) 32%. Protein kinases which were inhibited by more than 50% at 100 nM **7** are Flt4, Pim1, GSK3α, GSK3β, and MKK7β.

Table 1: Inhibition of angiogenesis and tumor-cell-induced neovascularization in developing zebrafish embryos.[a]

Compounds (amount)	Inhibition of angiogenesis (% defects/% survival)[b]	Tumor-induced neovascularization (% positive)[c]
DMSO	0/91 ± 2	78 ± 4
12 (5 μM)	0/86 ± 5	75 ± 3
7 (1 μM)	79 ± 5/90 ± 2	36 ± 1
7 (5 μM)	100 ± 0/91 ± 3	28 ± 3

[a] See the Supporting Information for experimental details. [b] Given are the percentages of embryos with defects in dorsal longitudinal anastomic vessels, intersegmental vessels or/and subintestinal veins formation after 72 hours postfertilization. Percentages of surviving embryos under the experimental conditions are also indicated. Three independent experiments were performed with 100 embryos each. No phenotypic differences were observed for the solvent control and the N-methylated compound compared to untreated embryos. [c] Given are the percentages of embryos with induced vessel formation at 24 hours postinjection of tumor cells. Two independent experiments were performed and 80 embryos were investigated for each concentration and compound. Nontransplanted zebrafish embryos do not show a similar formation of microvasculature from the subintestinal veins.

($IC_{50} = 125 \pm 23$ nM at 250 μM ATP). Thus, it can be concluded that the high selectivity of the organometallic complex **7** renders it a promising tool for investigating biological processes related to Flt4.

The receptor tyrosine kinase Flt4 plays essential roles in the development and maintenance of lymphatic vessels as well as in the development of the embryonic cardiovascular system.[9] In early mouse embryos it has been shown that a targeted inactivation of the Flt4 gene results in the formation of defective blood vessels.[13] Similarly, it has been demonstrated that Flt4 signaling is required for vasculogenesis and angiogenesis in the developing zebrafish.[14] We therefore tested the effect of complex **7** on angiogenesis and tumor-induced neovascularization in two zebrafish models.[15] Accordingly, transgenic zebrafish (*Danio rerio*) embryos in which the vascular system exhibits green fluorescence because of the expression of the green fluorescent protein (GFP) under an early endothelial promoter, were exposed to the organometallic compound **7**. The subsequent analysis with confocal fluorescence microscopy demonstrated that compound **7** strongly inhibits vessel formation with 79% and 100% of the zebrafish embryos being affected 3 days postfertilization at concentrations of 1 μM and 5 μM, respectively (Table 1 and Figure 4).

The induction of new blood vessels is an important process in tumor progression and we therefore evaluated the inhibitory effect of compound **7** on tumor-cell-induced angiogenesis, and we used an in vivo tumor xenograft angiogenesis assay in zebrafish embryos.[16,17] This neovascularization assay allows us to follow the induction of blood vessel formation by xenotransplanted proangiogenic human cancer cells, in this study transplanted human pancreatic tumor cells (PaTu-8998T cells), in real-time in living zebrafish and enables the quantification of neovascularization in vivo and in high resolution. Revealingly, our results show inhibitory effects of **7** on tumor-cell-induced angiogenesis. For example, compound **7**, when added to the water containing the zebrafish embryos at two nonlethal concentrations, strongly inhibited the induction of new microvasculature in the zebrafish neovascularization assay (Table 1). Figure 4 illustrates the effect of compound **7**: Whereas zebrafish embryos treated with DMSO show the typical tumor-cell-induced outgrowth

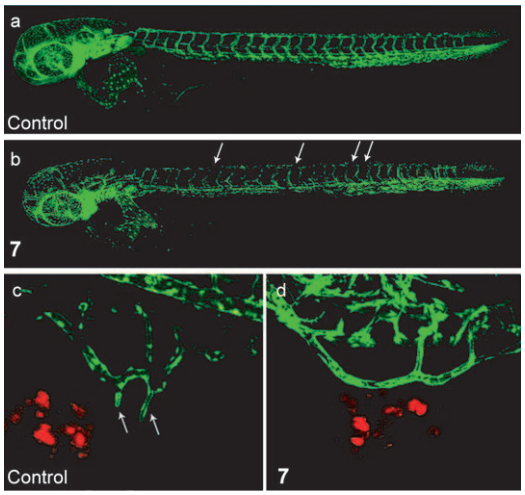

Figure 4. Effect of iridium compound **7** on angiogenesis and tumor-cell-induced neovascularization in transgenic zebrafish embryos exhibiting a green fluorescent vascular system. a,b) Angiogenesis assay: Examples of laser scanning confocal microscopy images shown at 3 days postfertilization of zebrafish embryos treated with (a) DMSO or (b) compound **7** at 5 μM. Vessel defects are marked with white arrows. c,d) Tumor xenotransplantation angiogenesis assay: Embryos were transplanted with human pancreatic cancer cells (red fluorescent as a result of CM-DiI staining) and treated with (c) DMSO control or (d) compound **7** at 5 μM and images were taken by dual-laser scanning confocal microscopy at 24 hours posttransplantation. The outgrowth of the subintestinal vein in the control experiment is marked with two white arrows and suppressed in the presence of compound **7**.

of the subintestinal vein (marked with two arrows in Figure 4c), the formation of new blood vessels is suppressed successfully in the presence of 5 μM of iridium compound **7** (Figure 4d).

Taken together, these data show that compound **7** has antiangiogenic properties in vivo and inhibits both, angiogenesis in developing zebrafish embryos as well as tumor-cell-induced angiogenesis. Importantly, the related organometallic complex **12** (Scheme 1), having an identical coordination sphere around the iridium(III) center but lacking the ability to inhibit protein kinases effectively because of a methylated maleimide moiety (Flt4: $IC_{50} = 1520 \pm 280$ nM at 100 μM ATP), does not show any effects at similar concentrations in these two zebrafish assays (Table 1). This pronounced difference in bioactivities between the organometallic compounds **7** and **12** strongly suggests that it is the inhibition of protein kinases, most likely Flt4, which is responsible for the in vivo bioactivity of the organometallic compound **7**.

Organometallic compounds are traditionally disregarded as molecular scaffolds for the design of druglike molecules or molecular probes owing to the fear of toxicity resulting from an incompatibility of metal–carbon bonds with the biological environment. However, as shown in Table 1, the organoiridium Flt4 inhibitor **7**, containing multiple Ir–C bonds, does not affect the survival of the zebrafish embryos. Furthermore, cellular proliferation experiments with Hela cells confirm the low cytotoxicity of **7** with HeLa cells not being affected significantly in the presence of 1 μM **7** over 24 hours (see the Supporting Information).

In conclusion, we here reported the first example of a protein kinase inhibitor based on an octahedral iridium complex scaffold, synthetically accessed in a stereoselective fashion through oxidative addition. The high in vitro selectivity, presumable as a result of the overall scaffold rigidity, combined with a lacking cytotoxicity and the distinct in vivo biological activity in two zebrafish model systems indicates that organoiridium complexes such as **7**, containing an octahedral metal center and multiple metal–carbon bonds, are falsely ignored as scaffolds for the development of enzyme inhibitors.

Received: February 4, 2010
Published online: April 30, 2010

Keywords: bioorganometallic chemistry · angiogenesis · flt4/vegfr3 · protein kinase inhibitor · iridium

[1] E. Meggers, *Curr. Opin. Chem. Biol.* **2007**, *11*, 287–292.
[2] For a recent account, see: E. Meggers, G. E. Atilla-Gokcumen, H. Bregman, J. Maksimoska, S. P. Mulcahy, N. Pagano, D. S. Williams, *Synlett* **2007**, 1177–1189.
[3] J. Maksimoska, L. Feng, K. Harms, C. Yi, J. Kissil, R. Marmorstein, E. Meggers, *J. Am. Chem. Soc.* **2008**, *130*, 15764–15765.
[4] Even the *trans* effect, which is frequently exploited for the synthesis of square-planar complexes, is more complicated in octahedral metal complexes and has been used to control the stereochemistry the ligand exchange reactions only occasionally. See, for example: B. J. Coe, S. J. Glenwright, *Coord. Chem. Rev.* **2000**, *203*, 5–80.
[5] J. Burgess, *Inorg. React. Mech.* **1972**, *2*, 140–195.
[6] Inert luminescent Ir^{III} complexes have been used as luminescent bioprobes. See, for example: a) T.-H. Kwon, J. Kwon, J.-I. Hong, *J. Am. Chem. Soc.* **2008**, *130*, 3726–3727; b) M. Yu, Q. Zhao, L. Shi, F. Li, Z. Zhou, H. Yang, T. Yia, C. Huang, *Chem. Commun.* **2008**, 2115–2117; c) K. K.-W. Lo, P.-K. Lee, J. S.-Y. Lau, *Organometallics* **2008**, *27*, 2998–3006.
[7] For bioactive Ir^{III} complexes, see: a) M. A. Scharwitz, I. Ott, R. Gust, A. Kromm, W. S. Sheldrick, *J. Inorg. Biochem.* **2008**, *102*, 1623–1630; b) M. Dobroschke, Y. Geldmacher, I. Ott, M. Harlos, L. Kater, L. Wagner, R. Gust, W. S. Sheldrick, A. Prokop, *ChemMedChem* **2009**, *4*, 177–187; c) M. Ali Nazif, J.-A. Bangert, I. Ott, R. Gust, R. Stoll, W. S. Sheldrick, *J. Inorg. Biochem.* **2009**, *103*, 1405–1414.
[8] J. U. Mondal, D. M. Blake, *Coord. Chem. Rev.* **1982**, *47*, 206–238.
[9] M. J. Karkkainen, T. V. Petrova, *Oncogene* **2000**, *19*, 5598–5605.
[10] For related oxidative addition reactions with $[Ir(bpy)(cod)]^+$ (bpy = 2,2′-bipyridine), see for example: G. Mestroni, A. Camus, G. Zassinovich, *J. Organomet. Chem.* **1974**, *73*, 119–127.
[11] T. Umemoto, S. Ishihara, *J. Am. Chem. Soc.* **1993**, *115*, 2156–2164.
[12] H. Bregman, P. J. Carroll, E. Meggers, *J. Am. Chem. Soc.* **2006**, *128*, 877–884.
[13] D. J. Dumont, L. Jussila, J. Taipale, A. Lymboussaki, T. Mustonen, K. Pajusola, M. Breitman, K. Alitalo, *Science* **1998**, *282*, 946–949.
[14] E. A. Ober, B. Olofsson, T. Mäkinen, S.-W. Jin, W. Shoji, G. Y. Koh, K. Alitalo, D. Y. R. Stainier, *EMBO Rep.* **2004**, *5*, 78–84.
[15] For recent examples of metal complexes with antiangiogenic properties, see: a) A. Vacca, M. Bruno, A. Boccarelli, M. Coluccia, D. Ribatti, A. Bergamo, S. Garbisa, L. Sartor, G. Sava, *Br. J. Cancer* **2002**, *86*, 993–998; b) I. Ott, B. Kircher, C. P. Bagowski, D. H. W. Vlecken, E. B. Ott, J. Will, K. Bensdorf, W. S. Sheldrick, R. Gust, *Angew. Chem.* **2009**, *121*, 1180–1184; *Angew. Chem. Int. Ed.* **2009**, *48*, 1160–1163; c) I. Ott, X. Qian, Y. Xu, D. H. W. Vlecken, I. J. Marques, D. Kubutat, J. Will, W. S. Sheldrick, P. Jesse, A. Prokop, C. P. Bagowski, *J. Med. Chem.* **2009**, *52*, 763–770.
[16] R. S. Kerbel, *N. Engl. J. Med.* **2008**, *358*, 2039–2049.
[17] a) S. Nicoli, M. Presta, *Nat. Protoc.* **2007**, *2*, 2918–2923; b) S. Nicoli, D. Ribatti, F. Cotelli, M. Presta, *Cancer Res.* **2007**, *67*, 2927–2931.

